

# Journal Pre-proof

Electrochemical SERS and SOERS in a single experiment: A new methodology for quantitative analysis

Sheila Hernandez, Juan V. Perales-Rondon, Aranzazu Heras, Alvaro Colina



PII: S0013-4686(19)32433-8

DOI: <https://doi.org/10.1016/j.electacta.2019.135561>

Reference: EA 135561

To appear in: *Electrochimica Acta*

Received Date: 17 October 2019

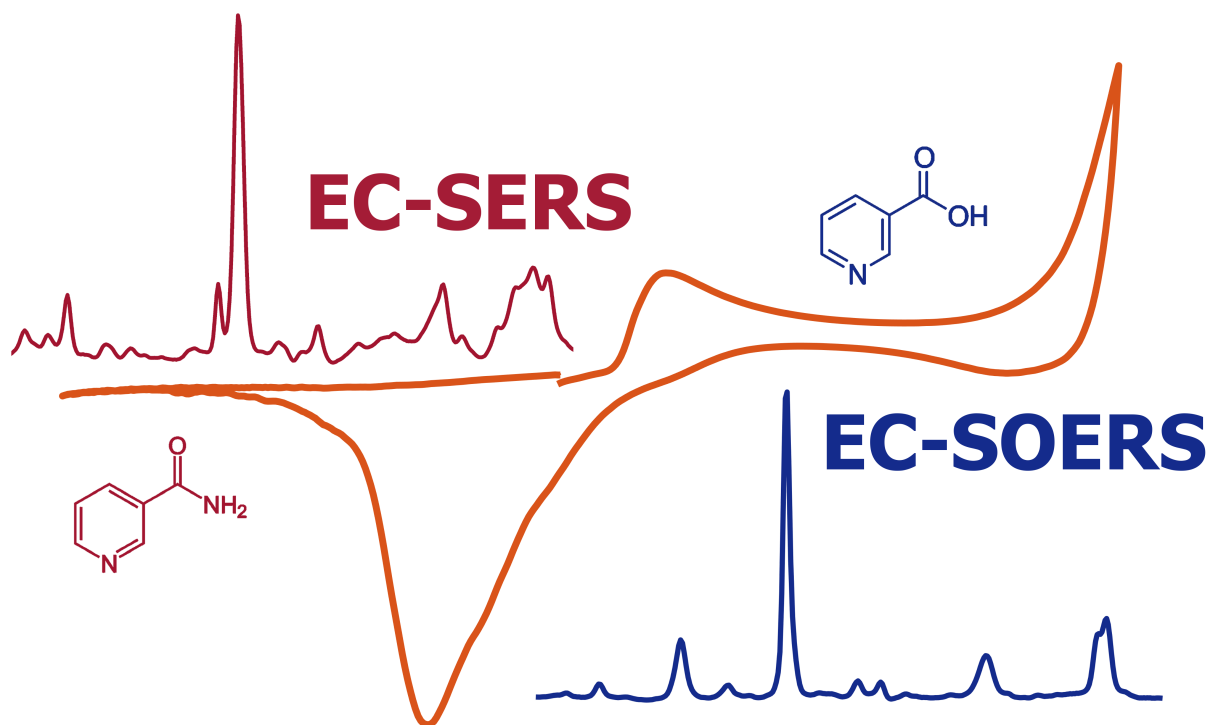
Revised Date: 5 December 2019

Accepted Date: 21 December 2019

Please cite this article as: S. Hernandez, J.V. Perales-Rondon, A. Heras, A. Colina, Electrochemical SERS and SOERS in a single experiment: A new methodology for quantitative analysis, *Electrochimica Acta* (2020), doi: <https://doi.org/10.1016/j.electacta.2019.135561>.

This is a PDF file of an article that has undergone enhancements after acceptance, such as the addition of a cover page and metadata, and formatting for readability, but it is not yet the definitive version of record. This version will undergo additional copyediting, typesetting and review before it is published in its final form, but we are providing this version to give early visibility of the article. Please note that, during the production process, errors may be discovered which could affect the content, and all legal disclaimers that apply to the journal pertain.

© 2019 Published by Elsevier Ltd.



Journal Pre-proof

**EXPERIMENT: A NEW METHODOLOGY FOR QUANTITATIVE  
ANALYSIS**

*Sheila Hernandez<sup>1</sup>, Juan V. Perales-Rondon\*<sup>1</sup>, Aranzazu Heras<sup>1</sup>, Alvaro Colina\*<sup>1</sup>.*

<sup>1</sup>Department of Chemistry, Universidad de Burgos, Pza. Misael Bañuelos s/n, E-09001 Burgos,  
Spain.

**Abstract**

In the present work, a new methodology which combines two different phenomena to enhance the Raman signal is used to resolve a mixture of two compounds with similar molecular structures. The use of Raman spectroelectrochemistry (Raman-SEC) allows us to collect simultaneously, with high time-resolution, the enhancement of the Raman signal of the compounds present in a sample during the electrochemical oxidation-reduction cycle (ORC) of a silver screen-printed electrode. During such ORC two different phenomena appears depending on the stage of the electrochemical modification of the silver substrate, which are known as electrochemical surface enhanced Raman scattering (EC-SERS) and electrochemical surface oxidation enhanced Raman scattering (EC-SOERS). This work is a proof of concept that demonstrates the advantage of using EC-SOERS and EC-SERS in a single experiment to resolve mixtures of similar molecules such as vitamin B3, which components are nicotinic acid and nicotinamide. Although the interaction between analytes and substrates influence a univariate calibration, the trilinear character of Raman-SEC makes possible to deconvolve such interactions and provide a good calibration curve for both, nicotinic acid and nicotinamide.

**Keywords:** EC-SERS; EC-SOERS; Raman spectroelectrochemistry; nicotinic acid; nicotinamide.

## 1. Introduction

Raman spectroscopy is a powerful technique to identify compounds and, due to the defined information that provides about the samples, this technique has a promising future for chemical analysis [1,2]. In spite of the rich information that can be obtained by Raman spectroscopy, one of the main drawbacks of this technique lays in the weakness of the Raman signal. To overcome such disadvantage, some methods to improve this signal have emerged over the last decades, with the so-called surface enhanced Raman scattering (SERS) being the most popular one. SERS implies the amplification of the Raman signal by several orders of magnitude [1,3–5], enabling its use in different fields like material characterization [6–8], surface science [9–12], chemical analysis [13,14], among others. Since its discovery in the 70's by Fleischmann [15], many researchers have made an extraordinary effort to obtain sensitive and reproducible SERS substrates. Because of that, a deep knowledge about the phenomenon has been achieved [3,4,16,17]. In fact, nowadays it is well-known that SERS effect occurs due to the contribution of two mechanisms: electromagnetic and chemical mechanisms [3,18–22].

In principle, a nanostructured metal surface is needed to obtain a good SERS substrate, which should exhibit plasmonic properties. In literature, it could be found different ways to obtain a SERS substrate. One of the most popular methods is the use of metal nanoparticles (Au, Ag, Cu) [17], which produce a significant enhancement of the Raman signal but usually is accompanied by a lack of reproducibility. Recently, the electrochemical roughening of screen printed electrodes of metal surfaces such as Ag, Au and Cu has been demonstrated to be very useful to improve this reproducibility, maintaining a very good sensitivity [23–26]. In this sense, the use of time resolved

Raman spectroelectrochemistry (TR-Raman-SEC) presents a clear advantage, because it allows obtaining a good and reproducible SERS substrate by electrochemical roughening, or oxidation-reduction cycle (ORC) as is known in literature. At the same time, TR-Raman-SEC enables the acquisition of Raman information with high time resolution during the metal roughening process, which enhances its usefulness as a versatile technique in SERS studies. Therefore, TR-Raman-SEC has become an interesting alternative for analysis and its applications are growing year by year [4,26,27].

In 2018, our research group discovered a new phenomenon equivalent to SERS, which provokes an enhancement of the Raman signal during the electrochemical oxidation of a silver electrode in a SEC experiment. This new phenomenon was denoted as electrochemical surface oxidation enhanced Raman scattering (EC-SOERS) [25], because the enhancement of the Raman signal only takes place when an anodic potential is applied to the electrode, that is to say, when the silver substrate is being electrochemically oxidized [25,28]. EC-SOERS has still been scarcely studied and, so far, the process has only been observed under particular electrolytic conditions ( $\text{HClO}_4$  + KCl electrolytic medium), using a silver electrode as metal substrate [28]. As far as we know, EC-SOERS occurs due to the contribution of two main effects [25]: (1) the electrochemical surface adsorption of the molecule at anodic potentials (due to the electrode polarization), and (2) the interaction of the molecule with the substrate ( $\text{Ag}^+/\text{AgCl}$  or  $\text{Ag}/\text{AgCl}$  nanostructures) [29–31] formed on the electrode surface at these anodic potentials. Compared with a classical EC-SERS experiment, where the SERS signal is particularly obtained at cathodic potentials (to avoid the damage of the nanostructured surface), in EC-SOERS the signal is exclusively registered at the electrochemical oxidation stage of the silver electrode. Moreover, a molecule can

exhibit SERS but not SOERS enhancement, or *vice versa*, depending on its chemical structure. These remarkable differences enable us to design new strategies for quantitative determination that could not be used under classic SERS conditions, opening new possibilities for chemical analysis. In this work, we propose to carry out the detection of two different molecules in a single experiment, taking into account their interaction with the substrates prepared at both, anodic and cathodic potentials. Thus, using Raman-SEC in particular electrolytic conditions ( $\text{HClO}_4/\text{KCl}$ ) in a silver electrode, it is possible to obtain a good substrate for both, EC-SERS and EC-SOERS, being even possible the detection and quantification of organic molecules that are only different in a functional group. This problem has been selected to illustrate the powerfulness of the methodology, but it could be also used for much simpler analytical problems.

Vitamin B3 has been selected as a proof of concept to demonstrate the capability of EC-SERS and EC-SOERS to detect and quantify two quite similar molecules in a single TR-Raman-SEC experiment. Vitamin B3 [32] can be found in two different forms, as nicotinic acid and/or nicotinamide. These two compounds have a similar structure (pyridine ring, Figure 1) with a different functional group as substituent, carboxylic acid for nicotinic acid and amide group for nicotinamide. This vitamin is particularly interesting in fields such as medicine, chemistry and biochemistry, because exhibits an important biological activity and its deficiency could cause several diseases. Vitamin B3 is an enzyme cofactor necessary for the synthesis of nicotinamide adenine dinucleotide (NAD) and nicotinamide adenine dinucleotide phosphate (NADP), molecules with a remarkable interest in the cellular metabolism [33]. Deficiency of this vitamin could cause pellagra, a disease characterized by a darkly pigmented skin rash, weakness, diarrhea, dermatitis and nervous disorders [34,35]. To prevent and treat such

disease, Vitamin B3 is used as oral supplement [36]. The Recommended Dietary Allowance (RDA) of this vitamin is 16 mg/day for men and 14 mg/day for women [37]. Most of commercial supplements use to contain enough vitamin B3 to fulfill the dietary requirements in an adult human. However, while nicotinamide has a tolerable upper intake level (UL) of 900 mg/day for adults, the nicotinic acid UL is only 10 mg/day. A dose higher of this UL may cause skin flushing [36,37]. Because of that, it is also important to quantify each of the components in Vitamin B3.

In the present work, a double and simultaneous determination of nicotinic acid and nicotinamide during a TR-Raman-SEC experiment is proposed. Using cyclic voltammetry (CV) as electrochemical technique, nicotinic acid is determined by EC-SOERS at anodic potentials, whereas nicotinamide is determined by EC-SERS, at cathodic potentials during an electrochemical ORC of a silver electrode. Using this Raman-SEC methodology is effortless to differentiate and determine, with high accuracy, these two analytes with such a similar structure.

## **2. Experimental section.**

### **2.1. Reagents and Materials.**

Nicotinamide (99+ %, reagent, ACROS Organics), nicotinic acid (99.5 %, reagent, ACROS Organics), perchloric acid ( $\text{HClO}_4$ , 60 %, reagent, Sigma-Aldrich) and potassium chloride (KCl, 99+ %, reagent, ACROS Organics) were used. All solutions were prepared using ultrapure water obtained from a Millipore DirectQ purification system provided by Millipore (18.2 M $\Omega$  cm resistivity at 25 °C).

### **2.2. Instrumentation.**

In situ TR-Raman-SEC was performed by using a customized SPELEC RAMAN instrument (Metrohm-DropSens), which integrates a laser source of 785 nm. Laser Power in all experiments was 80 mW ( $254 \text{ W}\cdot\text{cm}^{-2}$ ). This instrument was connected to a bifurcated reflection probe (DRP-RAMANPROBE, Metrohm-DropSens). A customized Raman spectroelectrochemical cell was employed to be used with screen-printed electrodes and DropView SPELEC software (Metrohm-DropSens) was used to control the instrument [24].

### **2.3. Time-resolved Raman spectroelectrochemistry experiments.**

During the TR-Raman-SEC experiment, DropView SPELEC software was used to collect simultaneously Raman spectra and the electrochemical data [24]. CV was chosen as electrochemical technique to carry out the electrochemical ORC of the silver electrode. CVs were carried out between vertex potentials  $-0.40 \text{ V}$  and  $+0.40 \text{ V}$ , starting at  $-0.025 \text{ V}$  in the anodic direction and at a scan rate of  $0.02 \text{ V}\cdot\text{s}^{-1}$ . Raman spectra were collected with an integration time of 1 s. All the experiments were performed with silver screen-printed electrodes (Ag-SPE, DRP-C013, Metrohm-DropSens). In order to obtain a reproducible experiment, a conditioning of the Ag-SPE was carried out. This consists of applying a CV with the same potential window of the experiment described previously, using an electrolytic solution of  $0.1 \text{ M HClO}_4 + 0.01 \text{ M KCl}$ . After that, the Ag-SPE was rinsed with ultrapure water and homogenized with the sample solution before the SEC experiment. This procedure was repeated for each sample in both, the calibration and the test samples.

## **3. Results and discussion.**

### **3.1. Spectroelectrochemistry characterization of nicotinamide and nicotinic acid.**

Before carrying out the simultaneous determination of these two molecules, Raman-SEC experiments of each analyte were performed to explore the evolution of the Raman spectra along the electrochemical experiment. Figure 1 shows the Raman spectra for  $5 \cdot 10^{-3}$  M nicotinic acid and 0.01 M nicotinamide in 0.1 M  $\text{HClO}_4$  + 0.01 M KCl at the maximum signal during a SEC experiment (at the oxidation stage of silver electrode for nicotinic acid, +0.39 V, and at the reduction stage of silver electrode for nicotinamide, -0.31 V). It is important to clarify that these specific electrolytic conditions (0.1 M  $\text{HClO}_4$  + 0.01 M KCl) were chosen based on some previous works conducted in our research group [25,28,38]. In those works, the enhancement of the Raman signal at anodic potentials was observed under  $\text{Cl}^-$  concentrations between 0.01 M and 0.005 M, and at pH 1. These  $\text{Cl}^-$  concentrations allows both, the formation of proper plasmonic structures and the electrochemical adsorption of the analyte at anodic potentials. This special behavior of the enhancement in the Raman signal was coined in the literature as EC-SOERS phenomenon.

For a better comparison of the Raman spectra see Figure S1 in the SI, the band assignment is provided in Table S1 and S2 in the SI. Raman spectra from concentrated solutions of both nicotinic acid and nicotinamide are also shown in the SI (Figure S2). Compared with the respective SERS/SOERS spectra, Raman spectra are very similar, being the differences probably due to the interaction between the analyte and the metallic surface in each case. The Raman spectra are in good agreement with the data found in literature for nicotinic acid and nicotinamide [2,34,39]. The two spectra present the main peak around  $1034 \text{ cm}^{-1}$  for nicotinic acid and  $1037 \text{ cm}^{-1}$  for nicotinamide, related to the ring breathing mode.

Figure 1

It is noteworthy that other peaks can differentiate both molecules, two bands for nicotinic acid ( $848\text{ cm}^{-1}$  and  $1602\text{ cm}^{-1}$ ) and other two for nicotinamide ( $999\text{ cm}^{-1}$  and  $1432\text{ cm}^{-1}$ ). However, under the experimental conditions used in EC-SERS and EC-SOERS experiments and taking into account the low concentrations of the samples tested (see Figure S3 and S4 in the SI), those differences become so small that cannot be used for quantitative purposes.

The evolution of the Raman signal at a characteristic Raman shift of the studied molecule plotted with respect to the applied potential helps to understand the effect of potential on the Raman signal of nicotinamide and nicotinic acid (Figure 2). In order to simplify the terminology, this plot will be called voltaRamagram along the manuscript. Figure 2 shows the cyclic voltammograms registered compared with the individual voltaRamagram of each analyte during a SEC experiment, selecting the Raman shift where the main peak of each molecule emerges. The evolution of the Raman peak for nicotinic acid ( $1034\text{ cm}^{-1}$ ) appears exclusively at anodic potentials, *i.e.*, during the electrochemical oxidation stage of the silver electrode (blue line, Figure 2A). This behavior has been previously reported as a new unexpected phenomenon denoted as EC-SOERS, as was aforementioned. As previous works describe [25,28], the enhancement of Raman signal is taking place probably due to the combination of two simultaneous phenomena: (1) the formation of  $\text{Ag}^+/\text{AgCl}$  or  $\text{Ag}/\text{AgCl}$  nanostructures on the electrode surface, which can interact with the molecule, and (2) the electrochemical adsorption of the molecule due to the electrode polarization at anodic potentials [25,28] (see CV in Figure 2 and S5 to follow the electrochemistry process). Thus, EC-SOERS

depends strongly on the potential and on the electrolytic conditions, and it provides a good and reproducible enhancement of the Raman signal, being especially useful for analytical applications. On the contrary, nicotinamide reach the maximum of the Raman intensity ( $1037\text{ cm}^{-1}$ ) at cathodic potentials, where the reduction of silver chloride generated during the oxidation scan is taking place (garnet line, Figure 2B). Clearly, the different behavior observed during the experiment can be used to separate the contribution of the two analytes. Finally, EC-SOERS occurs under specific electrolytic conditions ( $0.1\text{ M HClO}_4 + 0.01\text{ M KCl}$  electrolytic medium), under which the formation of  $\text{Ag}^+/\text{AgCl}$  or  $\text{Ag}/\text{AgCl}$  nanostructures is favored. It is worth noting that the analytical enhancement factors for the substrates prepared under these experimental conditions are quite different for the two phenomena, being  $1 \cdot 10^4$  for EC-SOERS and  $4 \cdot 10^2$  for EC-SERS. The latter suggests that the electrolytic conditions favors the formation of a proper SOERS substrate more than a SERS one.

As was stated above, there are other Raman peaks in each molecule that follow the same trend of the main bands. Figures S6 and S7 show the voltaRamangrams of three characteristic bands for nicotinic acid ( $848\text{ cm}^{-1}$ ,  $1034\text{ cm}^{-1}$  and  $1602\text{ cm}^{-1}$ ) and other three for nicotinamide ( $999\text{ cm}^{-1}$ ,  $1037\text{ cm}^{-1}$  and  $1432\text{ cm}^{-1}$ ), respectively. Raman bands at  $1034$  and  $1037\text{ cm}^{-1}$  for nicotinic acid and nicotinamide, respectively, are the best from a quantitative point of view because of the highest sensitivity that allows us to achieve a better limit of detection of these molecules.

From the voltaRamangrams, it can be concluded that nicotinic acid has a typical EC-SOERS behavior [25,28] while nicotinamide present a characteristic EC-SERS signal. It is noteworthy that nicotinic acid shows a higher Raman enhancement than nicotinamide in the present conditions, demonstrating the capability of EC-SOERS to amplify the

Raman signal and the similarity of the two enhancement processes. Surely, the experimental conditions used for nicotinamide were not the best ones to obtain the highest SERS enhancement. However, a compromise between EC-SOERS and EC-SERS has to be achieved. Under these experimental conditions, a suitable SOERS and SERS substrate can be obtained, with the two phenomena being clearly observed.

Figure 2

### **3.2. Quantitative determination of nicotinamide and nicotinic acid in aqueous solution using TR-Raman-SEC and univariate calibration models.**

In order to evaluate the capability of prediction of TR-Raman-SEC as analytical method to determine nicotinic acid and nicotinamide in the same test solution, different samples were prepared with different concentrations of nicotinic acid and nicotinamide to obtain the calibration curves. It should be highlighted that calibration samples do not increase at the same concentration for the two analytes but are randomly prepared along the corresponding concentration range. Additionally, a test sample (ts) was also prepared with nominal concentration of both analytes. The concentrations of the two analytes in each standard sample and of the test sample are listed in Table 1. All samples were prepared in 0.1 M HClO<sub>4</sub> and 0.01 M KCl, which is a suitable electrolytic medium to carry out the double determination by EC-SOERS and EC-SERS.

**Table 1.** Concentrations of nicotinic acid and nicotinamide in the standard and test samples for the calibration curves.

<b>Sample</b>	<b>Nicotinic acid (Vit. B3H) / mM</b>	<b>Nicotinamide (Vit. B3N) / mM</b>
<b>s01</b>	<b>0.5</b>	<b>5</b>
<b>s02</b>	<b>2</b>	<b>20</b>
<b>s03</b>	<b>4</b>	<b>1</b>
<b>s04</b>	<b>6</b>	<b>16</b>
<b>s05</b>	<b>8</b>	<b>12</b>
<b>s06</b>	<b>10</b>	<b>8</b>
<b>ts</b>	<b>5</b>	<b>10</b>

The integration time at which each Raman spectra was registered during the Raman-SEC experiment was 1 s. It should be noted that longer integration times would help to improve the sensitivity of the method but decreases the time resolution of the process taking place on the electrode surface. One calibration model was constructed for each analyte, selecting the characteristic Raman band for each molecule at the potential where takes the highest value during the CV. These Raman intensity values were systematically acquired at the same potential, +0.39 V (cathodic direction) for nicotinic acid and -0.31 V (cathodic direction) for nicotinamide during the Raman-SEC experiment (see Figure S8). It should be noted that at these two selected potentials, the adsorption of the compounds, considering the maximum Raman intensity, is the highest for the two analytes. Thus, at +0.39 V the adsorption of nicotinic acid is favored over nicotinamide, and vice versa at -0.31 V.

Figure 3 shows the calibration curves for nicotinic acid (A) and nicotinamide (B). To construct such curves, the Raman intensity of the main peak at +0.39 V (cathodic direction) for nicotinic acid and at -0.31 V (cathodic direction) for nicotinamide during CV for each analyte was plotted against the concentration for each sample. Blue dotted

line is obtained by fitting the responses with the concentrations of one analyte in presence of low concentrations of the other. As can be observed in Figure 3A (calibration curve for nicotinic acid, samples s01, s03, s06), samples s02, s04, s05 and ts does not follow a linear relationship with concentration. Interestingly, those samples have the higher concentration of nicotinamide (see Table 1) and, consequently, the Raman signal presents a positive deviation. On the other hand, in Figure 3B (calibration curve for nicotinamide, samples s01, s02, s03), it can be seen that s04, s05, s06 and ts have the higher positive influenced in the Raman signal, as in the case of the calibration curve for nicotinic acid. Again, these samples contain the higher concentrations of nicotinic acid (see Table 1).

Based on these results, there is a clear interaction between the two analytes and the substrates used to enhance the Raman signal, which makes more complex the determination of these components in a mixture. As was mentioned before, the presence of high concentrations of one molecule provokes a positive deviation in the Raman intensity registered. There are two possible reasons for such a behavior. The first one is the possibility of a change in the amount or type of the electrogenerated plasmonic nanostructure because of the presence of a specific molecule, in such a way that, when the amount of nicotinamide increases, the Raman signal for nicotinic acid is higher and *vice versa*. However, although this effect could be possible, it is expected that when the two analytes are in a high concentration (sample s06), the Raman signal would present also a positive deviation, but it is not the case. In consequence, this first hypothesis is discarded.

Figure 3

The second reason lays in the possibility of molecular co-adsorption. As is well known in literature, SERS effect has a narrow dependence with the distance of the molecule to the plasmonic surface [3]. Additionally, EC-SOERS has demonstrated to depend on the adsorption of the molecule to the electrode surface during the silver surface oxidation [25,28]. Based on this assertion, it is clear that the molecular adsorption plays a key role in the observation of EC-SERS and EC-SOERS signal. Thus, as the adsorption depends on the applied potential, it is expected that the adsorption of nicotinic acid would be favored at the oxidation stage of the silver electrode (because the electrochemical adsorption of the conjugated base of the acid is favored at these potentials), whereas at the reduction stage of the silver substrate, nicotinamide adsorption is induced. It is possible that when the amount of nicotinamide is high, this molecule is co-adsorbed with nicotinic acid at anodic potentials, provoking a higher enhancement of the Raman signal and the consequent positive deviation in the calibration curve of the nicotinic acid. Conversely, when the amount of nicotinic acid increases, a co-adsorption with nicotinamide is possible at cathodic potentials, which could be responsible for the positive deviation of such samples in the calibration curve for nicotinamide.

We can conclude that because of the interaction with the substrates of both, nicotinic acid and nicotinamide, presumably due to a co-adsorption of them (particularly present at higher concentrations of the analyte), it is not possible to carry out a quantitative determination of both molecules using EC-SERS and EC-SOERS with a univariate calibration model. Therefore, one alternative to overcome such a problem is to use multivariate analysis that allows unraveling the interactions between the components of

the system thanks to the trilinear character of TR-Raman-SEC, being possible to determine, with high accuracy, both components.

### **3.3. Quantitative determination of nicotinamide and nicotinic acid using EC-SERS, EC-SOERS and multivariate calibration.**

One of the main advantages of SEC is the high amount of information about the compounds in solution that is obtained in a single experiment. This information can be used to deconvolve complex chemical processes. Statistical tools are very useful for extracting the quantitative information contained in a SEC experiment. Particularly, SEC data provide a cube of data formed by the Raman intensity at the different Raman Shifts for all the applied potentials. Therefore, trilinear data can be analyzed with very powerful multivariate analysis techniques. Particularly, in this work, N-way partial least squares (N-way-PLS) [40,41] has been selected because it is able to deal with matrix effects. Additionally, multilinear models are much simpler compared with unfolding ones, because they use fewer parameters and are, hence, preferable due to its simplicity [41]. Finally, one of the main advantages of the method consists of the simpler chemical interpretation of the models compared with unfold-PLS [41]. As was aforementioned, because of the trilinear character of the data obtained by Raman-SEC experiments, and thanks to the combination of EC-SERS and EC-SOERS phenomena, the resolution of mixtures of several components is possible using N-way-PLS.

A previous exploration of the most suitable electrolytic conditions was carried out before performing the SEC experiments to resolve the mixture of nicotinic acid and nicotinamide. Figure S9 shows the calibration curves obtained after adjusting an N-way-PLS model to a series of SEC experiments obtained using 0.1 M HClO<sub>4</sub> + 5·10<sup>-3</sup> M KCl with calibration samples with nominal concentrations as those listed in Table 1. In

this model, the spectra from  $650\text{ cm}^{-1}$  to  $1650\text{ cm}^{-1}$  obtained during the whole potential scan, from  $-0.40$  to  $+0.40\text{ V}$  starting at  $-0.025\text{ V}$  in the anodic direction, were employed. Three components were used to obtain the model. From the results it is clear that determination of nicotinic acid can be carried out using  $5 \cdot 10^{-3}\text{ M KCl}$ , obtaining a good prediction of the test sample, demonstrating the good analytical performance of EC-SOERS. However, at this concentration of KCl, uncertainty of nicotinamide determination is higher because of the low SERS signal. It is clear that such electrolytic conditions ( $5 \cdot 10^{-3}\text{ M KCl}$ ) are not the optimal ones to obtain a good SERS substrate, and the signal obtained in EC-SERS is not good enough to achieve the best quantitative determination.

Previous studies demonstrated that the optimal concentrations of KCl for EC-SOERS can be found between  $5 \cdot 10^{-3}\text{ M}$  and  $0.01\text{ M}$  [28]. Moreover, when  $\text{Cl}^-$  concentration is increased, the SERS substrate yields a better enhancement of the Raman signal. This fact has been previously described in studies about the optimal concentrations of KCl to obtain good SERS signals using colloidal silver [42,43]. In brief, a compromise situation needs to be solved, with a concentration of  $\text{Cl}^-$  high enough to obtain a good SERS substrate, but at the same time, a suitable  $\text{Cl}^-$  concentration to obtain a SOERS substrate in the same Raman-SEC experiment. A value of  $0.01\text{ M KCl}$  was selected for a good determination of the two analytes in a single experiment.

As has been stated above, an N-way-PLS model was constructed using three components obtained from the spectral data measured along the whole Raman-SEC experiment. The univariate models showed that the concentration of one of the analytes in the sample shows a clear influence on the other. Multivariate model not only allows us to construct good calibration curves but also helps to explain the effect of each

analyte on the other. This influence can be clearly observed by analyzing the loadings related to the Raman Spectra (Figure 4A) and the loadings related to the voltamogram (Figure 4B). Loadings for each component are moved in the ordinate axis for a clear understanding of Figure 4. As can be seen in Figure 4A, the three components are related to: 1) nicotinic acid (blue line) in which the characteristics bands of the acid are seen; 2) nicotinamide (red line) in which the spectrum of this compound is observed and 3) a mixture of the two spectra (yellow line) is clearly observed. This assignment is confirmed when Figure 4B is analyzed. In this figure, the blue line, corresponding to nicotinic acid, shows a clear EC-SOERS behavior, with the Raman intensity increasing in the anodic region of the scan, that is to say, during the electrochemical oxidation of the silver electrode. On the contrary, the red line, corresponding to nicotinamide, increases in the cathodic region where the SERS substrate is formed. The third component (yellow line) can be related with the influence of each analyte on the other. Nicotinamide initially yields signal at the beginning of the EC-SOERS region but decreases when nicotinic acid is adsorbed. Thus, when nicotinic acid concentration is large enough, this compound seems to be co-adsorbed with nicotinamide yielding a larger Raman intensity than the expected as has been seen in univariate calibration.

Figure 4

Therefore, although EC-SOERS and EC-SERS processes are different, as can be deduced by the signals of the two components, the spectral response is not completely

independent because compounds with similar structure exhibit a clear influence in the optical signal, being mandatory to use multivariate statistics to resolve the mixture.

For the N-way-PLS model constructed for the mixture of nicotinic acid and nicotinamide, a good linear correlation was observed, as can be noticed by the  $R^2$  value of 0.97 for nicotinic acid (Figure 5A) and 0.98 for nicotinamide (Figure 5B). The data also show a low dispersion, which denotes a high precision. The concentration of each compound was estimated for the test sample with an error lower than 10 %, which represents a high accuracy (8.7 % for both, nicotinic acid and nicotinamide). It is important to notice that one of the main advantages of this method is the high sensitivity, evidenced in the possibility to differentiate between two samples of very similar concentration, even in presence of a clear interference of the other form of vitamin B3.

Figure 5

#### 4. Conclusions.

A new methodology for Raman quantitative analysis has been proposed. The new methodology is based on the electrochemical generation of a SERS and SOERS substrate in a single experiment. Thanks to the combination of EC-SERS and EC-SOERS with multivariate statistical tools, the resolution of a complex mixture has been achieved, demonstrating the capability of the methodology to resolve the components of vitamin B3 (nicotinic acid and nicotinamide). This proof of concept demonstrates the advantages of using simultaneously EC-SOERS and EC-SERS to resolve complex

mixtures of compounds, even with very similar chemical structures. Univariate calibration was influenced by the interaction between the analytes but N-way-PLS was able to deconvolve such interactions and provide good calibration curves for both, nicotinic acid and nicotinamide, allowing the determination of a test sample with high accuracy. This methodology opens new gates to design analytical strategies in order to resolve mixtures in a simple and fast way. The high amount of information obtained in a single TR-Raman-SEC experiments helps not only to resolve complex mixtures but also to understand the complex chemical processes taking place at the electrode/solution interface.

## 5. Acknowledgment

Authors acknowledge the financial support from Ministerio de Economía y Competitividad (Grants CTQ2017-83935-R-AEI/FEDERUE), Junta de Castilla y León (Grant BU033-U16 and BU297P18) and Ministerio de Ciencia, Innovación y Universidades (RED2018-102412-T). J.V.P-R. thanks JCyL for his postdoctoral fellowship (Grant BU033-U16). S.H. wish to thank JCyL and European Social Fund for her predoctoral grant.

## 6. Appendices

Appendices contain the following supplementary material: Raman bands assignments, normal Raman spectra of nicotinic acid and nicotinamide, Raman spectra at different concentrations, CV of the electrolytic medium, voltaRamagram at different Raman shifts and the representation of an N-way-PLS model for a set of data (PDF).

## 7. References

- [1] B. Sharma, R.R. Frontiera, A.-I. Henry, E. Ringe, R.P. Van Duyne, SERS: Materials, applications, and the future, *Mater. Today*. 15 (2012) 16–25. doi:10.1016/S1369-7021(12)70017-2.
- [2] S.M. Park, K. Kim, M.S. Kim, Adsorption of picolinic and nicotinic acids on a silver sol surface investigated by Raman spectroscopy, *J. Mol. Struct.* 344 (1995) 195–203. doi:10.1016/0022-2860(94)08439-O.
- [3] P.L. Stiles, J.A. Dieringer, N.C. Shah, R.P. Van Duyne, Surface-Enhanced Raman Spectroscopy, *Annu. Rev. Anal. Chem.* 1 (2008) 601–626. doi:10.1146/annurev.anchem.1.031207.112814.
- [4] S. Schlücker, Surface-enhanced raman spectroscopy: Concepts and chemical applications, *Angew. Chemie - Int. Ed.* 53 (2014) 4756–4795. doi:10.1002/anie.201205748.
- [5] U.K. Sur, Surface-enhanced Raman spectroscopy, *Resonance*. 15 (2010) 154–164. doi:10.1007/s12045-010-0016-6.
- [6] J.A. Dieringer, A.D. McFarland, N.C. Shah, D.A. Stuart, A. V. Whitney, C.R. Yonzon, M.A. Young, X. Zhang, R.P. Van Duyne, Surface enhanced Raman spectroscopy: New materials, concepts, characterization tools, and applications, *Faraday Discuss.* 132 (2006) 9–26. doi:10.1039/b513431p.
- [7] H.J. Butler, L. Ashton, B. Bird, G. Cinque, K. Curtis, J. Dorney, K. Esmonde-White, N.J. Fullwood, B. Gardner, P.L. Martin-Hirsch, M.J. Walsh, M.R. McAinsh, N. Stone, F.L. Martin, Using Raman spectroscopy to characterize biological materials, *Nat. Protoc.* 11 (2016) 664–687.

- doi:10.1038/nprot.2016.036.
- [8] Y. Zhang, S. Zhao, J. Zheng, L. He, Surface-enhanced Raman spectroscopy (SERS) combined techniques for high-performance detection and characterization, *TrAC - Trends Anal. Chem.* 90 (2017) 1–13.  
doi:10.1016/j.trac.2017.02.006.
- [9] M. Musiani, J.-Y. Liu, Z.-Q. Tian, Applications of Electrochemical Surface-Enhanced Raman Spectroscopy (EC-SERS), in: *Dev. Electrochem.*, John Wiley & Sons, Ltd, Chichester, UK, 2014: pp. 137–162.  
doi:10.1002/9781118694404.ch8.
- [10] Z.Q. Tian, J.S. Gao, X.Q. Li, B. Ren, Q.J. Huang, W.B. Cai, F.M. Liu, B.W. Mao, Can surface Raman spectroscopy be a general technique for surface science and electrochemistry?, *J. Raman Spectrosc.* 29 (1998) 703–711.  
doi:10.1002/(SICI)1097-4555(199808)29:8<703::AID-JRS286>3.0.CO;2-L.
- [11] Z.C. Zeng, S.C. Huang, D.Y. Wu, L.Y. Meng, M.H. Li, T.X. Huang, J.H. Zhong, X. Wang, Z.L. Yang, B. Ren, Electrochemical Tip-Enhanced Raman Spectroscopy, *J. Am. Chem. Soc.* 137 (2015) 11928–11931.  
doi:10.1021/jacs.5b08143.
- [12] S.R. Smith, J.J. Leitch, C. Zhou, J. Mirza, S.-B. Li, X.-D. Tian, Y.-F. Huang, Z.-Q. Tian, J.Y. Baron, Y. Choi, J. Lipkowski, Quantitative SHINERS Analysis of Temporal Changes in the Passive Layer at a Gold Electrode Surface in a Thiosulfate Solution, *Anal. Chem.* 87 (2015) 3791–3799. doi:10.1021/ac504433t.
- [13] C. Zong, M. Xu, L.J. Xu, T. Wei, X. Ma, X.S. Zheng, R. Hu, B. Ren, Surface-Enhanced Raman Spectroscopy for Bioanalysis: Reliability and Challenges, *Chem. Rev.* 118 (2018) 4946–4980. doi:10.1021/acs.chemrev.7b00668.

- [14] O.E. Eremina, A.A. Semenova, E.A. Sergeeva, N.A. Brazhe, G. V Maksimov, T.N. Shekhovtsova, E.A. Goodilin, I.A. Veselova, Surface-enhanced Raman spectroscopy in modern chemical analysis: advances and prospects, *Russ. Chem. Rev.* 87 (2018) 741–770. doi:10.1070/RCR4804.
- [15] M. Fleischmann, P.J. Hendra, A.J. McQuillan, Raman spectra of pyridine adsorbed at a silver electrode, *Chem. Phys. Lett.* 26 (1974) 163–166. doi:10.1016/0009-2614(74)85388-1.
- [16] A. Balčytis, Y. Nishijima, S. Krishnamoorthy, A. Kuchmizhak, P.R. Stoddart, R. Petruškevičius, S. Juodkazis, From Fundamental toward Applied SERS: Shared Principles and Divergent Approaches, *Adv. Opt. Mater.* 6 (2018) 1800292. doi:10.1002/adom.201800292.
- [17] Z.-Q. Tian, B. Ren, D.-Y. Wu, Surface-Enhanced Raman Scattering: From Noble to Transition Metals and from Rough Surfaces to Ordered Nanostructures, *J. Phys. Chem. B.* 106 (2002) 9463–9483. doi:10.1021/jp0257449.
- [18] S.-Y. Ding, E.-M. You, Z.-Q. Tian, M. Moskovits, Electromagnetic theories of surface-enhanced Raman spectroscopy, *Chem. Soc. Rev.* 46 (2017) 4042–4076. doi:10.1039/C7CS00238F.
- [19] S.-Y. Ding, J. Yi, J.-F. Li, B. Ren, D.-Y. Wu, R. Panneerselvam, Z.-Q. Tian, Nanostructure-based plasmon-enhanced Raman spectroscopy for surface analysis of materials, *Nat. Rev. Mater.* 1 (2016) 16021–16036. doi:10.1038/natrevmats.2016.21.
- [20] T. Itoh, K. Yoshida, V. Biju, Y. Kikkawa, M. Ishikawa, Y. Ozaki, Second enhancement in surface-enhanced resonance Raman scattering revealed by an analysis of anti-Stokes and Stokes Raman spectra, *Phys. Rev. B - Condens.*

- Matter Mater. Phys. 76 (2007) 1–5. doi:10.1103/PhysRevB.76.085405.
- [21] D.Y. Wu, X.M. Liu, S. Duan, X. Xu, B. Ren, S.H. Lin, Z.Q. Tian, Chemical enhancement effects in SERS spectra: A quantum chemical study of pyridine interacting with copper, silver, gold and platinum metals, *J. Phys. Chem. C*. 112 (2008) 4195–4204. doi:10.1021/jp0760962.
- [22] A. Campion, J.E. Ivanecky, C.M. Child, M. Foster, On the Mechanism of Chemical Enhancement in Surface-Enhanced Raman Scattering, *J. Am. Chem. Soc.* 117 (1995) 11807–11808. doi:10.1021/ja00152a024.
- [23] D.-Y. Wu, J.-F. Li, B. Ren, Z.-Q. Tian, Electrochemical surface-enhanced Raman spectroscopy of nanostructures, *Chem. Soc. Rev.* 37 (2008) 1025–1041. doi:10.1039/b707872m.
- [24] D. Martín-Yerga, A. Pérez-Junquera, M.B. González-García, J. V. Perales-Rondon, A. Heras, A. Colina, D. Hernández-Santos, P. Fanjul-Bolado, Quantitative Raman spectroelectrochemistry using silver screen-printed electrodes, *Electrochim. Acta*. 264 (2018) 183–190. doi:10.1016/j.electacta.2018.01.060.
- [25] J. V. Perales-Rondon, S. Hernandez, D. Martin-Yerga, P. Fanjul-Bolado, A. Heras, A. Colina, Electrochemical surface oxidation enhanced Raman scattering, *Electrochim. Acta*. 282 (2018) 377–383. doi:10.1016/j.electacta.2018.06.079.
- [26] D. Martín-Yerga, A. Pérez-Junquera, M.B. González-García, D. Hernández-Santos, P. Fanjul-Bolado, Towards single-molecule in situ electrochemical SERS detection with disposable substrates, *Chem. Commun.* 54 (2018) 5748–5751. doi:10.1039/C8CC02069H.

- [27] L. Zhao, J. Blackburn, C.L. Brosseau, Quantitative Detection of Uric Acid by Electrochemical-Surface Enhanced Raman Spectroscopy Using a Multilayered Au/Ag Substrate, *Anal. Chem.* 87 (2015) 441–447. doi:10.1021/ac503967s.
- [28] J. V. Perales-Rondon, S. Hernandez, A. Heras, A. Colina, Effect of chloride and pH on the electrochemical surface oxidation enhanced Raman scattering, *Appl. Surf. Sci.* 473 (2019) 366–372. doi:10.1016/j.apsusc.2018.12.148.
- [29] Z. Gan, A. Zhao, M. Zhang, D. Wang, W. Tao, H. Guo, D. Li, M. Li, Q. Gao, A facile strategy for obtaining fresh Ag as SERS active substrates, *J. Colloid Interface Sci.* 366 (2012) 23–27. doi:10.1016/J.JCIS.2011.09.052.
- [30] N. Zhao, X. Fei, X. Cheng, J. Yang, Synthesis of silver/silver chloride/graphene oxide composite and its surface-enhanced Raman scattering activity and self-cleaning property, *IOP Conf. Ser. Mater. Sci. Eng.* 242 (2017) 12002. doi:10.1088/1757-899X/242/1/012002.
- [31] L. Dawn, W. Jian, X. Houwen, S. Xu, L. Fan-chen, Enhancement origin of SERS from pyridine adsorbed on AgCl colloids, *Spectrochim. Acta Part A Mol. Spectrosc.* 43 (1987) 379–382. doi:10.1016/0584-8539(87)80120-4.
- [32] K.L. Bogan, C. Brenner, Nicotinic Acid, Nicotinamide, and Nicotinamide Riboside: A Molecular Evaluation of NAD<sup>+</sup> Precursor Vitamins in Human Nutrition, *Annu. Rev. Nutr.* 28 (2008) 115–130. doi:10.1146/annurev.nutr.28.061807.155443.
- [33] W. Ying, NAD<sup>+</sup>/NADH and NADP<sup>+</sup>/NADPH in Cellular Functions and Cell Death: Regulation and Biological Consequences, *Antioxid. Redox Signal.* 10 (2008) 179–206. doi:10.1089/ars.2007.1672.

- [34] T. Pal, V. Anantha Narayanan, D.L. Stokes, T. Vo-Dinh, Surface-enhanced Raman detection of nicotinamide in vitamin tablets, *Anal. Chim. Acta.* 368 (1998) 21–28. doi:10.1016/S0003-2670(98)00192-5.
- [35] K.L. Bogan, C. Brenner, Nicotinic Acid, Nicotinamide, and Nicotinamide Riboside: A Molecular Evaluation of NAD<sup>+</sup> Precursor Vitamins in Human Nutrition, *Annu. Rev. Nutr.* 28 (2008) 115–130.  
doi:10.1146/annurev.nutr.28.061807.155443.
- [36] C. Minto, M.G. Vecchio, M. Lamprecht, D. Gregori, Definition of a tolerable upper intake level of niacin: a systematic review and meta-analysis of the dose-dependent effects of nicotinamide and nicotinic acid supplementation, *Nutr. Rev.* 75 (2017) 471–490. doi:10.1093/nutrit/nux011.
- [37] C. Agostoni, Scientific Opinion on Dietary Reference Values for niacin, *EFSA J.* 12 (2014) 3759. doi:10.2903/j.efsa.2014.3759.
- [38] S. Hernandez, J. V. Perales-Rondon, A. Heras, A. Colina, Determination of uric acid in synthetic urine by using electrochemical surface oxidation enhanced Raman scattering, *Anal. Chim. Acta.* 1085 (2019) 61–67.  
doi:10.1016/j.aca.2019.07.057.
- [39] J.L. Castro, J.F. Arenas, M.R. Lopez-Ramirez, J. Soto, J.C. Otero, Surface-enhanced Raman scattering of picolinamide, nicotinamide, and isonicotinamide: Unusual carboxamide deprotonation under adsorption on silver nanoparticles, *J. Colloid Interface Sci.* 396 (2013) 95–100. doi:10.1016/j.jcis.2013.01.050.
- [40] C.A. Andersson, R. Bro, The N-way Toolbox for MATLAB, *Chemom. Intell. Lab. Syst.* 52 (2000) 1–4. doi:10.1016/S0169-7439(00)00071-X.

- [41] R. Bro, Multiway calibration. Multilinear PLS, *J. Chemom.* 10 (1996) 47–61.  
doi:10.1002/(SICI)1099-128X(199601)10:1<47::AID-CEM400>3.0.CO;2-C.
- [42] Y.S. Li, J. Cheng, Y. Wang, Surface-enhanced Raman spectra of dyes and organic acids in silver solutions: Chloride ion effect, *Spectrochim. Acta - Part A Mol. Biomol. Spectrosc.* 56 (2000) 2067–2072. doi:10.1016/S1386-1425(00)00268-7.
- [43] A. Otto, A. Bruckbauer, Y.. Chen, On the chloride activation in SERS and single molecule SERS, *J. Mol. Struct.* 661–662 (2003) 501–514.  
doi:10.1016/j.molstruc.2003.07.026.

**Figures caption**

**Figure 1.** EC-SOERS spectrum for  $5 \cdot 10^{-3}$  M nicotinic acid (blue line) and EC-SERS spectrum for 0.01 M nicotinamide (garnet line) in 0.1 M HClO<sub>4</sub> + 0.01 M KCl electrolytic medium, registered during a SEC experiment at the maximum of signal for each analyte (+0.39 V for nicotinic acid and -0.31 V for nicotinamide).

**Figure 2.** VoltaRamagram of (A)  $5 \cdot 10^{-3}$  M nicotinic acid at 1034 cm<sup>-1</sup> (blue line) and (B) 0.01 M nicotinamide at 1037 cm<sup>-1</sup> (garnet line) in comparison with the corresponding CV (black lines) on a silver screen printed electrode. Electrolytic medium: 0.1 M HClO<sub>4</sub> + 0.01 M KCl. Signals registered during a TR-Raman-SEC experiment where the cyclic voltammetry was chosen as electrochemical technique. Scan rate 0.02 V·s<sup>-1</sup>.

**Figure 3.** Univariate calibration models for nicotinic acid (A) and nicotinamide (B). Raman intensity at 1034 cm<sup>-1</sup> is taken at +0.39 V (cd) for nicotinic acid and at 1037 cm<sup>-1</sup> and -0.31 V (cd) for nicotinamide during the TR-Raman-SEC experiment. Blue dotted line is obtained by fitting the responses with the concentrations of each analyte in presence of different concentration of the other compound. Garnet points are related to standard calibration samples shown in Table S3 and green points to the test sample.

**Figure 4.** Loadings related to (A) the spectra and (B) the voltaRamagrams obtained with an N-way-PLS model with three components. Ordinate for each component is shifted for a clearer representation

**Figure 5.** Concentrations predicted by the N-way-PLS versus real concentrations of the analyte for (A) nicotinic acid and (B) nicotinamide. Green point is a test sample.

Fig1.

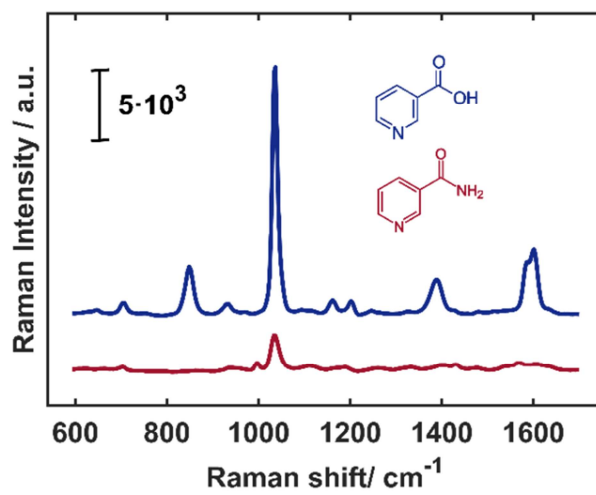


Fig.2

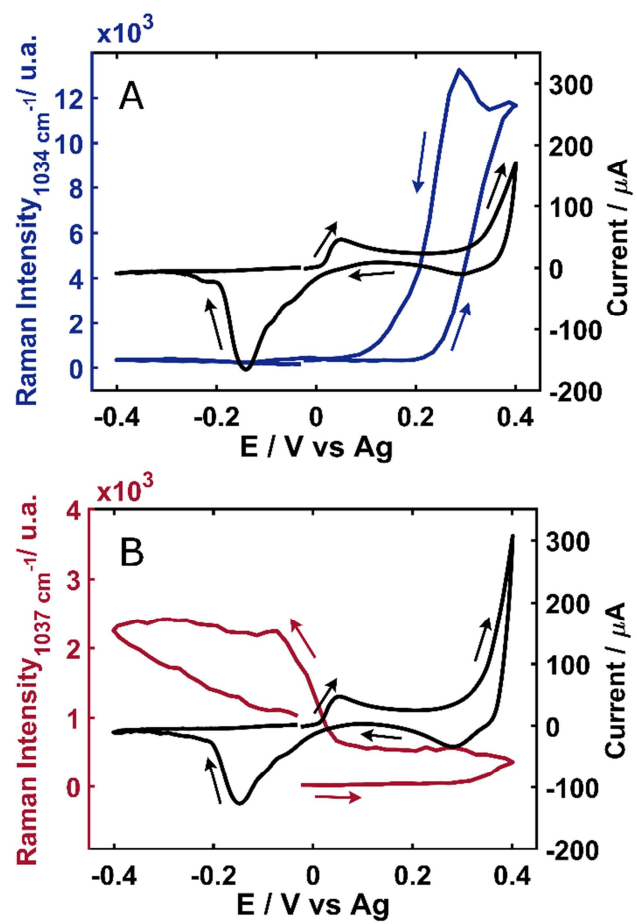


Fig.3

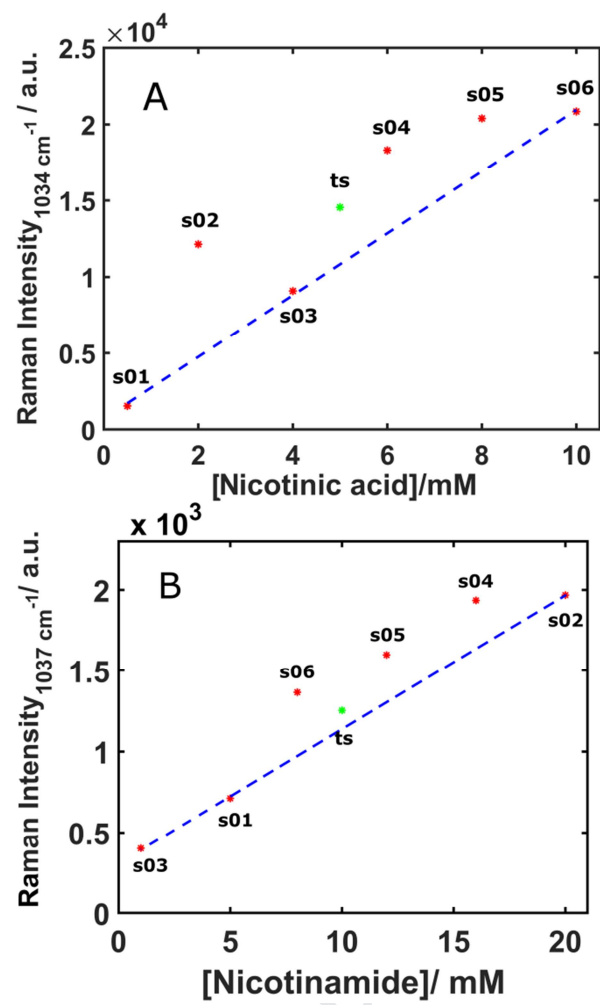


Fig.4

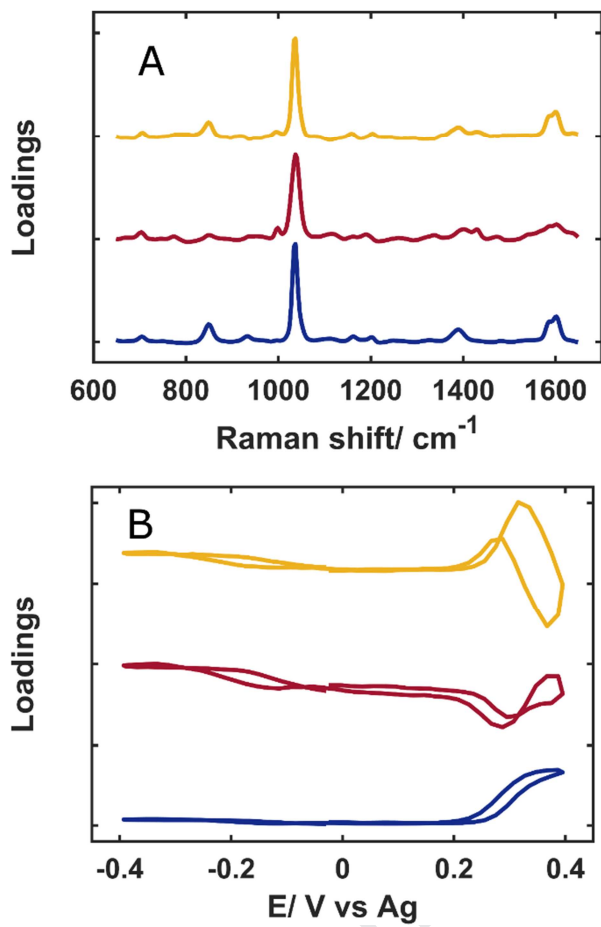
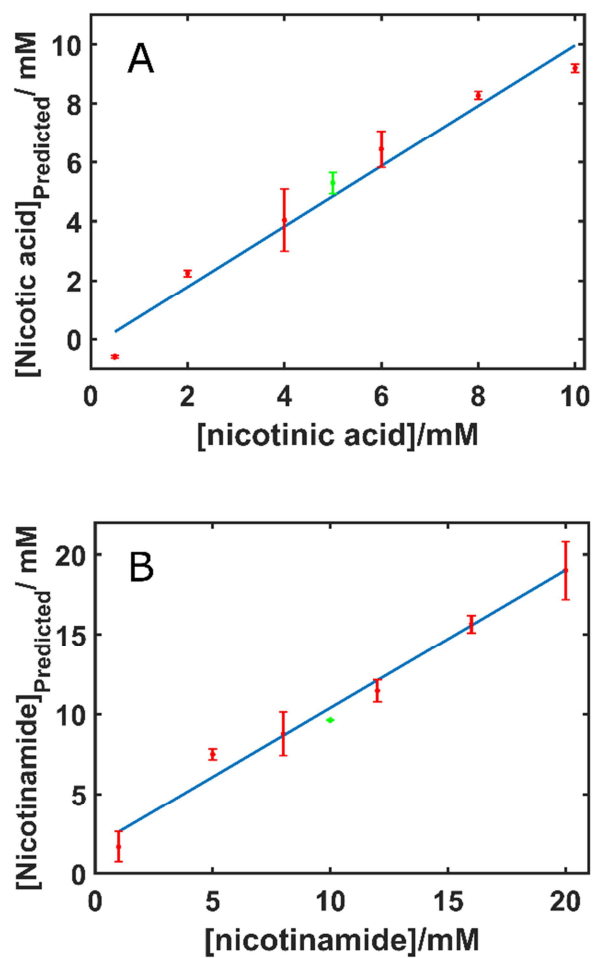


Fig. 5



S.H and J.P-R. carried out the experiments. S.H., J.P-R., A.H and A.C. contributed to the design and implementation of the research, to the analysis of the results and to the writing of the manuscript.

Journal Pre-proof

## AUTHOR DECLARATION

Journal Pre-proof

We wish to confirm that there are no known conflicts of interest associated with this publication and there has been no significant financial support for this work that could have influenced its outcome.

We confirm that the manuscript has been read and approved by all named authors and that there are no other persons who satisfied the criteria for authorship but are not listed. We further confirm that the order of authors listed in the manuscript has been approved by all of us.

We confirm that we have given due consideration to the protection of intellectual property associated with this work and that there are no impediments to publication, including the timing of publication, with respect to intellectual property. In so doing we confirm that we have followed the regulations of our institutions concerning intellectual property.

We understand that the Corresponding Author is the sole contact for the Editorial process (including Editorial Manager and direct communications with the office). He/she is responsible for communicating with the other authors about progress, submissions of revisions and final approval of proofs. We confirm that we have provided a current, correct email address which is accessible by the Corresponding Author and which has been configured to accept email from acolina@ubu.es

Signed by all authors as follows:

Alvaro Colina  
Aranzazu Heras  
Juan Victor Perales-Rondon  
Sheila Hernandez